Eur. Phys. J. B (2022)95:147
https://doi.org/10.1140/epjb/s10051-022-00411-z

THE EUROPEAN PHYSICAL JOURNAL B

Regular Article - Solid State and Materials

Quantum phase transition in skewed ladders: an entanglement entropy and fidelity study

Sambunath Das[1,2], Dayasindhu Dey[1,3], S. Ramasesha[1], and Manoranjan Kumar[2,a]

[1] Solid State and Structural Chemistry Unit, Indian Institute of Science, Bangalore 560012, India
[2] S. N. Bose National Centre for Basic Sciences, Block-JD, Sector-III, Salt lake, Kolkata 700106, India
[3] UGC-DAE Consortium for Scientific Research, University Campus, Khandwa Road, Indore 452001, India

Received 4 July 2022 / Accepted 22 August 2022

Abstract. Entanglement entropy (EE) of a state is a measure of correlation or entanglement between two parts of a composite system and it may show appreciable change when the ground state (GS) undergoes a qualitative change in a quantum phase transition (QPT). Therefore, the EE has been extensively used to characterise the QPT in various correlated Hamiltonians. Similarly fidelity also shows sharp changes at a QPT. We characterized the QPT of frustrated antiferromagnetic Heisenberg spin-1/2 systems on 3/4, 3/5 and 5/7 skewed ladders using the EE and fidelity analysis. It is noted that all the non-magnetic to magnetic QPT boundary in these systems can be accurately determined using the EE and fidelity, and the EE exhibits a discontinuous change, whereas fidelity shows a sharp dip at the transition points. It is also noted that in case of the degenerate GS, the unsymmetrized calculations show wild fluctuations in the EE and fidelity even without actual phase transition, however, this problem is resolved by calculating the EE and the fidelity in the lowest energy state of the symmetry subspaces, to which the degenerate states belong.

1 Introduction

Quantum phase transition (QPT) involves a qualitative change in the nature of the ground state (GS) in the phase space of the Hamiltonian parameters. The prerequisite for a Hamiltonian to exhibit QPT is that it should consist of noncommuting terms. In this case the quantum fluctuations drive the QPT. In 1-D and 2-D Hamiltonians the fluctuations are dominant, making them viable candidates to exhibit QPT. Many interesting and exotic quantum phases observed include the dimer phase [1–10], spin liquid phase [4–6,8,9,11], charge density waves [12–15], spin density waves [16–18], vector chiral phase [2,19–21], the valence bond solid [22–24] and topological phases [25–28], to name a few. The QPT is different from the classical or thermal phase transition in which phase transition is driven by the competition between energy and thermal entropy at finite temperature. Quantum fluctuations are dominant in confined systems like one, quasi-one or two dimensional systems and lead to many interesting quantum phases. In a quantum system the EE which indirectly measures the correlation between different parts of the system is expected to change in QPT. The extent of entanglement depends on Hamiltonian parameters such as system geometry, competing interaction parameters, magnetic and electric fields.

Effective low dimensional systems such as spin chains and spin ladders are of enduring interest for the past many decades. Fundamentally different spectral gaps in spin-1/2 and spin-1 chains predicted by Haldane, spin-Peierls' distortion in spin-1/2 chains predicted from theory, and occurrence of magnetization plateaus in spin ladders have all been observed experimentally [29–41]. Thus, most theoretical predictions of spin chains have been vindicated by experiments, mostly in molecular systems and magnetically low-dimensional systems characterized by strong exchange in one direction and much weaker exchange in orthogonal directions [42]. In fact, experimentally, there is evidence of systems [43] which belong to different regions of the quantum phase diagram in the well studied J_1- J_2-δ model of spin chains, where J_1 is the first neighbour exchange interaction, J_2 is the second neighbour exchange interaction and δ is the dimerization in the nearest neighbour exchange strength.

Belonging to the class of spin ladders is a class of skewed ladders where one or more rung bonds in the unit cell is slanted. This ladder system can also be mapped into zigzag ladders with periodically missing bonds as shown in Fig. 1. The skewed ladder is classified as n/m ladder where n and m are the ring sizes of adjacent rings in the ladder. These systems, in our

[a] e-mail: manoranjan.kumar@bose.res.in (corresponding author)

Published online: 09 September 2022

opinion, are realizable in concatenated transition metal complexes. This class of systems show a very interesting quantum phase diagram as a function of the ratio of the rung exchange (J_1) to the nearest neighbour leg exchange (J_2). Depending upon this ratio n/m and J_1/J_2 and system size, the skewed ladders show remarkable switching in the GS spin, exhibit bond order wave, spin density wave and chiral vector phases [44]. The Heisenberg antiferromagnetic (HAF) spin-1/2 system on 5/7, 3/4, 3/5 and 5/5 skewed ladders shows interesting magnetic and non-magnetic QPT in the parameter space of the rung and the leg spin exchange constants [44,45]. Recent work on HAF spin-1 on 5/7 [46], 3/4 and 3/5 [47] skewed ladders has also shown existence of similar magnetic and non-magnetic phase transitions. The quantum phases of HAF spin-1/2 system on 3/4, 5/5 and 3/5 skewed ladders studied at finite external axial magnetic field B are found to show various magnetic plateau phases which follow the Oshikawa, Yamanaka, and Affleck (OYA) [48] rule, in the $B - J_1 - J_2$ parameter space.

In general correlation functions, energy crossovers, GS symmetry changes and local order parameters are studied to characterize the QPT. However, hidden order like topological properties can not be detected by conventional procedures. Therefore, to study the long range correlations in the system and to characterize the phase boundaries sharply, we have studied the entanglement properties of this system. Where entanglement does not show sharp features, fidelity of the GS is a useful tool for determining the phase boundary. The QPT of frustrated J_1-J_2 model has been characterised using EE in earlier studies [49]. Simillarly the QPT of XXZ model has been studied using the fidelity as a property obtained from exact diagonalization and density matrix renormalization group methods [50]. The fidelity approach to characterize QPT is reviewed in [51].

We find that fidelity is very sensitive to changes in the GS and shows sharp changes even when the spin gap vs J_1/J_2 plots show only a change in the slope or when there is a cross over in the two low-lying excited states. When there is symmetry breaking, the fidelity in one of the subspaces shows a sharp change while in another subspace there is no change. This allows us to identify the symmetry before and after a quantum phase transition. In this work, we follow the changes in EE and fidelity of different skewed spin-1/2 ladders. We mainly focus on exact diagonalization studies of these ladders. We also employ symmetries such as the conservation of the z-component of total spin, S_z, and the reflection symmetry at degeneracies to follow changes in EE and fidelity. We find that in the 3/4 skewed ladder, EE shows sharp changes at the critical value of J_1. Fidelity also shows a similar sharp changes and we can identify the critical J_1 value very accurately. In the skewed ladders 3/5 and 5/7, both EE and fidelity show sharp changes and the critical J_1 values for QPT can be determined highly accurately. In what follows, we discuss the results of our studies on the 3/4, 3/5 and 5/7 ladder systems and show how both EE and fidelity can be used to accurately find critical J_1 values at the transition points.

This paper is divided into five sections. In Sect. 2 we provide a brief introduction to entanglement entropy and fidelity. We then present the model Hamiltonian and numerical methods in Sect. 3. The results are discussed in Sect. 4 under three subsections. The summary of our results are presented in Sect. 5.

2 Entanglement entropy and fidelity

Entanglement entropy (EE) has been studied extensively from a quantum information perspective due to the promise that quantum computing holds. It has also been shown in many studies that EE is a useful tool for studying phase transition in quantum systems. Given two subsystems A and B and spanning Hilbert spaces H_A and H_B with full system Hilbert space $H = H_A \times H_B$, we can always find an orthonormal bases $\{\phi_A\}$ and $\{\phi_B\}$ such that any state $|\psi_{AB}\rangle$ in the Hilbert space belonging to H, can be expressed as

$$|\psi_{AB}\rangle = \sum_{i,j} \alpha_{ij} |\phi_i\rangle_A |\phi_j\rangle_B. \tag{1}$$

The reduced density matrix of the subsystem B is given by

$$\rho_B = Tr_A \left(|\psi_{AB}\rangle\langle\psi_{AB}| \right), \tag{2}$$

and the jj'^{th} matrix element of the reduced density matrix ρ_B is,

$$(\rho_B)_{jj'} = \sum_i \alpha_{ij} \alpha^*{}_{ij'}. \tag{3}$$

If the eigenvalues of ρ_B are λ_i then we can define EE in many different ways. If we restrict ourselves to extensivity of entropy, i.e. $S_{AB} = S_A + S_B$, we can define entropy of a state in two ways. In condensed matter physics, the widely used entropy is the von Neumann entropy which is given by [52]

$$S = -\sum_i \lambda_i \log_2 \lambda_i, \tag{4}$$

where $\lambda_i{}'$s are the eigenvalues of the reduced density matrix. Von Neumann entropy is the generalization of the classical Shannon entropy. Another entropy function which is Rényi entropy $S^R_{A,\alpha}$ is defined as [53]

$$S^R_{A,\alpha} = \frac{1}{1-\alpha} \log \left[\sum_i (\rho_i^A)^\alpha \right] \tag{5}$$

where α can take values between 0 and ∞. Rényi entropy reduces to von Neumann entropy in the limit

$\alpha \to 1$ and it is maximum when $\alpha = 0$ and minimum when $\alpha \to \infty$.

In this work, we employ von Neumann entropy to analyze the QPT as von Neumann entropy is the most widely used entropy to study the QPT. We also restrict ourselves to equal sizes of the subsystems A and B as von Neumann entropy is maximum in this case. In frustrated one-dimensional spin chains, which are known as the $J_1 - J_2$ chains, the GS EE cannot identify the critical J_2 value (J_{2c}) below which the system is gapless and above which the system is gapped. However, the GS EE can identify the Majumdar-Ghosh point which is not surprising since the GS corresponds to nearest neighbor singlets [54]. The J_{2c} is correctly identified from EE when the J_2 corresponding to crossing of the EE of the first excited triplet and the second singlet is extrapolated from finite size calculations to the thermodynamic limit [54]. EE has also been studied in spin ladders and it has been shown that the area law of entanglement is valid upto seven legs [55].

A more sensitive property to follow QPT is fidelity and fidelity susceptibility. Fidelity ($F(\omega)$) at a parameter ω of the Hamiltonian is given by the overlap of the desired state of the Hamiltonian at ω with that in its neighborhood $\omega + \delta\omega$ i.e.

$$F(\omega) = \langle\psi(\omega)|\psi(\omega + \delta\omega)\rangle. \tag{6}$$

We can also define fidelity susceptibility $\chi(\omega)$ as

$$\chi(\omega) = \frac{2(1 - F(\omega))}{(\delta\omega)^2} \tag{7}$$

which follows from a Taylor series expansion of $F(\omega)$. It has been shown that fidelity of the GS in the $J_1 - J_2$ model can give accurate value of J_{2c} [56]. In the $J_1 - J_2$ model, the critical value of J_2 has also been determined by following the fidelity of the first excited state of short Heisenberg chains to determine $J_2(N)$ and extrapolating it to the thermodynamic limit $N \to \infty$ [57]. In the $J_1 - J_2 - \delta$ model, using EE, it is not possible to obtain the quantum phase diagram accurately; the EE contours show phase changes although phase boundries remain fuzzy. We have obtained the EE and fidelity of the 3/4, 3/5, and 5/7 skewed ladders; these systems show quantum phase transition for fixed next nearest neighbor exchange J_2 and varying nearest neighbor J_1 exchange.

3 Model Hamiltonian and numerical method

In our study, we consider a spin-1/2 model on 3/4, 3/5 and 5/7 skewed ladders as shown in Fig. 1a–c. The rung bond interaction is J_1 and the leg bond interaction is J_2. All the exchange interactions in the Hamiltonians we consider are antiferromagnetic in nature. The sites are numbered in such a way that the even numbered sites are on the top of the leg and odd numbers are on the bottom of the leg. The leg bond interaction J_2 is set to 1 and it defines the energy scale. The model Hamiltonian of 3/4 skewed ladder is written as

$$\begin{aligned} H_{3/4} = J_1 \sum_i \Big[& (\mathbf{S}_{i,1} \cdot \mathbf{S}_{i,2} + \mathbf{S}_{i,3} \cdot \mathbf{S}_{i,2}) \\ & + (\mathbf{S}_{i,4} \cdot \mathbf{S}_{i,5} + \mathbf{S}_{i,6} \cdot \mathbf{S}_{i,5}) \Big] \\ & + J_2 \sum_i \Big[(\mathbf{S}_{i,5} \cdot \mathbf{S}_{i+1,1} + \mathbf{S}_{i,6} \cdot \mathbf{S}_{i+1,2}) \\ & + \sum_{k=1}^{4} (\mathbf{S}_{i,k} \cdot \mathbf{S}_{i,k+2}) \Big], \end{aligned} \tag{8}$$

where i labels the unit cell and k the spins within the unit cell. The first term denotes the rung bond interaction and the second term denotes the leg bond interaction. Similarly, the model Hamiltonian for the 3/5 and 5/7 systems can be written as

$$\begin{aligned} H_{3/5} = J_1 \sum_i & (\mathbf{S}_{i,1} \cdot \mathbf{S}_{i,2} + \mathbf{S}_{i,3} \cdot \mathbf{S}_{i,2}) \\ & + J_2 \sum_i \Big(\mathbf{S}_{i,3} \cdot \mathbf{S}_{i+1,1} + \mathbf{S}_{i,4} \cdot \mathbf{S}_{i+1,2} \\ & + \sum_{k=1}^{2} \mathbf{S}_{i,k} \cdot \mathbf{S}_{i,k+2} \Big), \end{aligned} \tag{9}$$

and

$$\begin{aligned} H_{5/7} = J_1 \sum_i & (\mathbf{S}_{i,1} \cdot \mathbf{S}_{i,2} + \mathbf{S}_{i,4} \cdot \mathbf{S}_{i,5}) \\ & + J_2 \sum_i \Big(\mathbf{S}_{i,7} \cdot \mathbf{S}_{i+1,1} + \mathbf{S}_{i,8} \cdot \mathbf{S}_{i+1,2} \\ & + \sum_{k=1}^{6} \mathbf{S}_{i,k} \cdot \mathbf{S}_{i,k+2} \Big). \end{aligned} \tag{10}$$

We have carried out the computations using exact diagonalization technique on a system with 24 spin-1/2 sites, in all cases. We have employed cyclic boundary conditions and the EE computed is the von Neumann entropy. The environment and the system, both have equal number of sites, i.e. 12 sites. The reduced density matrix of the left half of the system is obtained by tracing over the right half of the system,

$$\rho_{LL'} = \sum_R C_{LR} C_{L'R} \tag{11}$$

where the GS wavefunction ψ_g is expressed in the direct product basis of the Fock space of the system (L) and the surroundings (R). The dimensionality of the Fock space of the system block, and hence the order of the density matrix is $2^{12} \times 2^{12}$ or 4096×4096. After

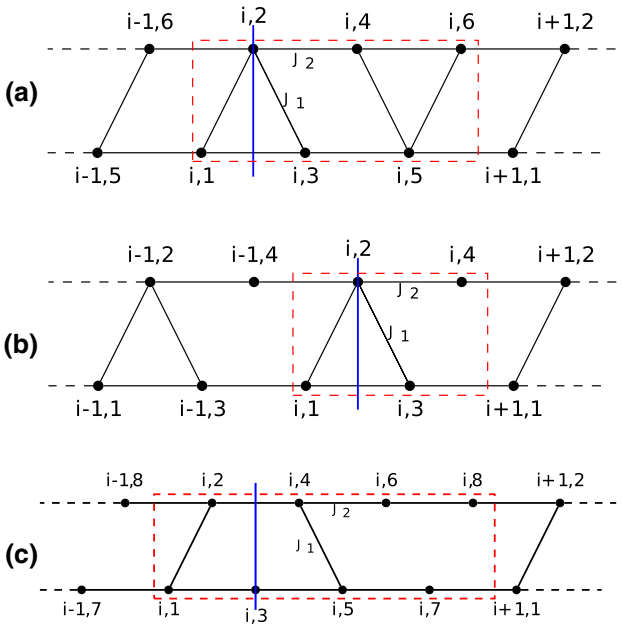

Fig. 1 Schematic diagram of **a** 3/4 skewed ladder, **b** 3/5 skewed ladder, and **c** 5/7 skewed ladder. The nearest neighbor or rung interaction is J_1 and the next-nearest neighbor (according to our numbering scheme) interaction is J_2. The sites on the top leg are even numbered and on the bottom leg are odd numbered. The unit cell for each ladder system is indicated by a rectangle with dashed red lines. The mirror plane for each ladder system is represented by a perpendicular blue line

obtaining all the eigenvalues $\{\lambda_i\}$ of the reduced density matrix, the von Neumann entropy is obtained from Eq. 4. We have computed the fidelity $F(J_1)$ of the state using the normalized ground states and Eq. 6. We have varied J_1 in very small steps of $\delta(= 0.001)$ near the quantum phase transitions obtained from the spin gap data. The spin gap Γ_l is defined as the energy gap between the lowest eigenstates $S_z = l$ and $S_z = 0$ manifolds, where S_z is the z-component of the total spin.

$$\Gamma_l = E_0(S_z = l) - E_0(S_z = 0), \tag{12}$$

where l is an integer. The GS spin $(S_G) = l$, for l that satisfies $\Gamma_l = 0$ and $\Gamma_{l+1} > 0$. The excitation gap Γ_σ at a fixed S_G between the lowest energy states in different reflection symmetry subspaces $\sigma(-)$ and $\sigma(+)$ is defined as

$$\Gamma_\sigma = E_0(S_G, \sigma(-)) - E_0(S_G, \sigma(+)). \tag{13}$$

The GS is in odd subspace $(\sigma(-))$ when $\Gamma_\sigma < 0$, even subspace $(\sigma(+))$ when $\Gamma_\sigma > 0$ and doubly degenerate when $\Gamma_\sigma = 0$.

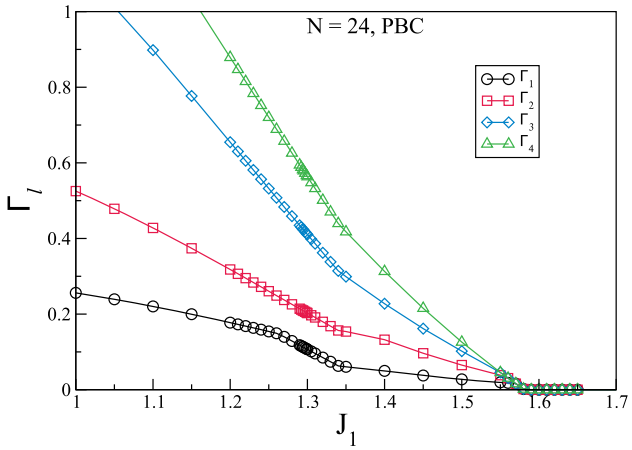

Fig. 2 Spin gaps Γ_l for a 3/4 skewed ladder of 24 spins with PBC shown as a function of J_1. The GS spin $S_G = 0$ for $J_1 < 1.581$ and $S_G = 4$ for $J_1 \geq 1.581$

4 Results and discussions

4.1 3/4 skewed ladder

This is the simplest of the skewed ladders to show a transition in the spin of the GS. However, there is a transition in the GS near $J_1 = 1.3$ which does not involve change in the GS spin. We notice in the Γ_l vs J_1 plot (Fig. 2) that there is a kink near $J_1 = 1.3$, but it is not possible to pin point the J_1 value at which this kink appears from the Γ_l plot. However, the EE shows a sharp change at $J_1 = 1.340$ and it is also seen more clearly in the fidelity, where it vanishes at $J_1 = 1.340$ but has a value of 1.0 for other J_1 values (Fig. 3). Closer examination of the full eigenvalue spectrum of the Hamiltonian shows that at this value of J_1, the singlet GS is doubly degenerate and there is a cross over from one singlet GS to another singlet GS. The transition to the highest spin states occurs sharply, when the GS spin changes to $S_G = 4$. The transition occurs at $J_1 = 1.581$ and there is a sharp drop in EE at this point. Fidelity also goes to zero at $J_1 = 1.581$ but assumes a value of 1, at the neighboring points. For larger system sizes, the level crossing method is used to calculate the transition points, and it has been reported that the transition points do not change significantly with system size (Ref. [44]). In this system, we have been able to determine the parameter at which the QPT occurs very accurately and we also find that there is a transition at $J_1 = 1.340$ which is not evident from the plots of the spin gaps.

4.2 3/5 skewed ladder

The GS of 3/5 skewed ladder is nonmagnetic for $J_1 < 2.026$ and the spin of the GS progressively increases from $S_G = 0$ to $S_G = 3$ form $J_1 = 2.026$ to 2.297 (Fig. 4a). The spin of the GS remains 3 as J_1 is increased further until $J_1 = 6.859$ and for $J_1 > 6.859$

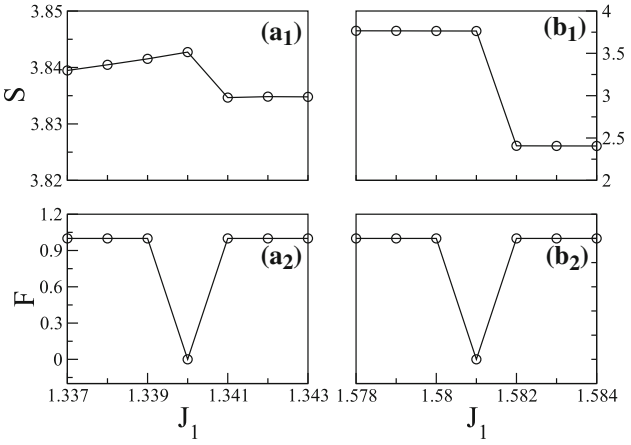

Fig. 3 The behaviour of EE (S) and fidelity (F) in the range $1.337 \leq J_1 \leq 1.343$ of a 3/4 skewed ladder with $N = 24$ spins are shown in (a_1) and (a_2) respectively. The EE changes abruptly and a sharp drop in fidelity occurs at $J_1 = 1.340$. At other values of J_1 fidelity is constant $(= 1)$. Simillary the behaviour of EE and fidelity in the range $1.578 \leq J_1 \leq 1.584$ are shown in (b_1) and (b_2). At $J_1 = 1.581$, the entropy changes and fidelity shows a sharp drop

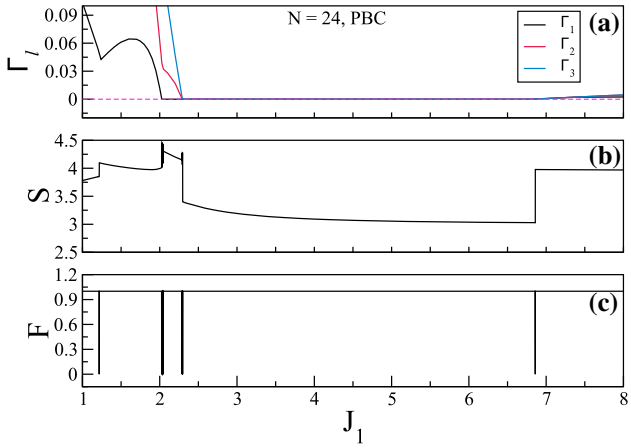

Fig. 4 **a** The spin gaps Γ_1, Γ_2 and Γ_3 are shown as a function of J_1 for N = 24 sites in a 3/5 skewed ladder with PBC. For $J_1 < 2.026$ and $J_1 > 6.859$, Γ_1 becomes 0 and the system shows nonmagnetic behaviour. In the region $2.026 \leq J_1 \leq 2.297$ the GS spin gradually changes from 0 to 3. **b** shows the EE and **c** shows the fidelity for the unsymmetrized GS as a function of J_1. The EE exhibits a discontinuous change, while fidelity shows a sharp drop at the transition points. The thick line near the vicinity of $J_1 = 2$ indicates many transitions both in EE and fidelity

the state reenters the nonmagnetic phase. EE and fidelity are shown in (Fig. 4b,c) over the entire range of our study, namely $1 \leq J_1 \leq 8$. In this ladder system, both EE and fidelity give the critical value of J_1 to be 1.217 (Fig. 5) and at this value of J_1 both the lowest energy state and first excited state are same upto third decimal space in $S_z = 0$ sector. Here again it is likely due to broken spatial symmetry in the GS. At $J_1 = 6.859$, we find a sharp transition in both EE and fidelity to the reentrant nonmagnetic phase.

For J_1 in the neighborhood of 2, fidelity and EE seem to indicate many transitions. The system has a reflection symmetry, as shown in Fig. 1b. The lowest energy states for $2.026 \leq J_1 \leq 2.046$ and $2.290 \leq J_1 \leq 2.296$, in the $\sigma(+)$ and $\sigma(-)$ manifold are degenerate. A linear combination of the degenerate states can lead to a broken symmetry state (see Ref. [44] for details). The intervals of J_1 for which the GS is doubly degenerate are shown in third column of Table 1. The EE of the eigenstate with symmetry shows a kink at $J_1 = 2.025$ below which the GS is in the $\sigma(-)$ space (σ is the reflection symmetry) and the EE in the $\sigma(+)$ space shows a kink at 2.046 (Fig. 6a). The fidelity of the GS in $\sigma(-)$ space show a drop at 2.025 and that in the $\sigma(+)$ space shows a drop at 2.046 (Fig. 6b). In the region between these values, the GS is doubly degenerate and any linear combination of these states is also an eigenstate and hence the EE and fidelity, calculated from unsymmetrized GS show wild fluctuations. For $2.290 \leq J_1 \leq 2.296$ the GS is degenerate. So the unsymmetrized calculation for both EE and fidelity shows wild fluctuations in this range of J_1. In symmetrized calculation, both the EE and fidelity change at $J_1 = 2.289$ and 2.296 (Fig. 6c,d). The $\mid \Gamma_\sigma \mid$ value vanishes in the interval $2.290 \leq J_1 \leq 2.296$. The GS below 2.290 has $\sigma(+)$

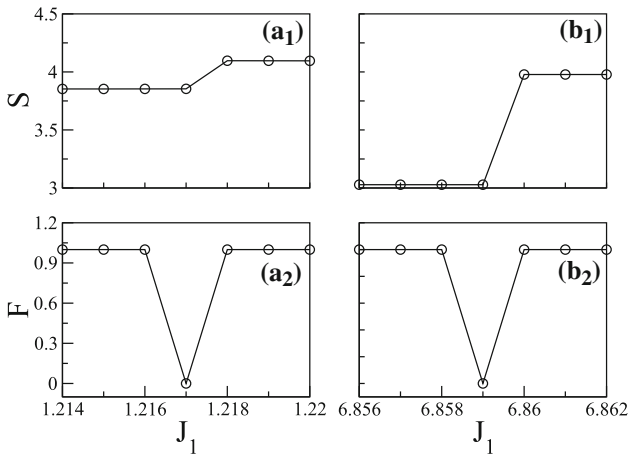

Fig. 5 The behaviour of EE (S) and fidelity (F) in the range of J_1 $(1.214 \leq J_1 \leq 1.22)$ of a 3/5 skewed ladder with $N = 24$ spins are shown in (a_1) and (a_2) respectively. The change in entropy and sharp drop in fidelity occurs at $J_1 = 1.217$. For other values of J_1 the fidelity is constant $(= 1)$. Simillary behaviour of the entropy and fidelity in the range of J_1 $(6.856 \leq J_1 \leq 6.862)$ are shown in (b_1) and (b_2) respectively. At $J_1 = 6.859$, the entropy changes and fidelity shows a sharp drop

symmetry whereas above 2.296 the GS has $\sigma(-)$ symmetry. Therefore fidelity for the $\sigma(+)$ subspace shows a sharp dip at $J_1 = 2.289$ and that of state $\sigma(-)$ shows a dip at $J_1 = 2.296$.

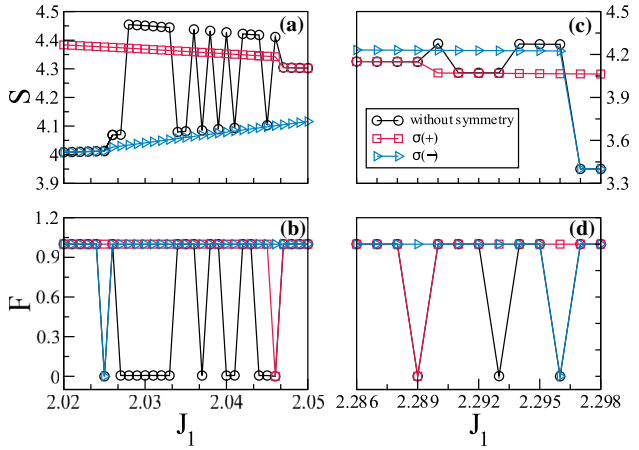

Fig. 6 The EE (S) and fidelity (F) of lowest energy states of a 3/5 skewed ladder for 24 sites with periodic boundary condition in different reflection symmetry subspaces ($(\sigma(+))$ and $(\sigma(-))$. Both the EE and fidelity for the unsymmetrized GS is represented by the black curve whereas for the symmetrised GS these are represented by the red and blue curves

4.3 5/7 skewed ladder

Among the skewed ladders we have studied, the 5/7 skewed ladder has by far the most interesting quantum phase transitions. For fixed $J_2 = J_1 = 1$, the GS spin of the system, S_G, increases with system size, a feature we have not observed in the other systems studied here. In this work, we focus on the EE and fidelity for a 24 spin 5/7 ladder with periodic boundary condition as a function of J_1. From the plot of spin gaps vs. J_1 (Fig. 7a) and earlier studies it is established that the GS switches from a singlet to a triplet at $J_1 = 1.427$. For $1.734 < J_1 < 1.872$ the GS of the system again becomes a singlet and for $J_1 > 1.872$ the GS changes spin, finally attaining a $S_G = 3$ for $J_1 \geq 2.355$. In (Fig. 7b, c) we show how the EE and fidelity varies as a function of J_1. At the first transition, both these quantities show a sharp change. In the region of the reentrant phase, the variations are violent. In the region $1.872 < J_1 < 2.176$, EE shows smooth variation and the fidelity also does not change. In this region the GS spin, $S_G = 1$. Although the S_G value continues to be 1 in the region $2.176 < J_1 < 2.355$, the EE as well as fidelity show very sharp changes. Finally beyond $J_1 = 2.355$, EE is almost constant and fidelity stays at 1.

The first transition from a singlet to a triplet is simple and the critical J_1 value can be pinned down both from EE and fidelity. This occurs at $J_1 = 1.427$. To understand the behavior at other values of J_1, we recognize that the system has a reflection symmetry perpendicular to the legs. So, the states of the system can be classified as $\sigma(+)$ or $\sigma(-)$ depending on the symmetry of the space in which the GS is found [44]. The range of J_1 for the lowest energy state in different subspaces is shown in Table 2. We see that the change in the spin of the GS from $S_G = 0$ to $S_G = 1$ at $J_1 = 1.427$ is also

Table 1 The interval of J_1 for the GS in different subspaces of a 3/5 skewed ladder with $N = 24$ spins. The first column represents the range of J_1 for which the GS is in $\sigma(+)$ subspace, the second column represents the GS in $\sigma(-)$ subspace. The third column gives the range of J_1 for which the difference between the lowest energies of two different subspaces is zero

$\sigma(+)$	$\sigma(-)$	$\mid \Gamma_\sigma \mid = 0$
$1 < J_1 \leq 1.217$ and $2.046 < J_1 < 2.290$	$1.217 \leq J_1 < 2.025$ and $J_1 > 2.296$	$2.026 \leq J_1 \leq 2.046$ and $2.290 \leq J_1 \leq 2.296$

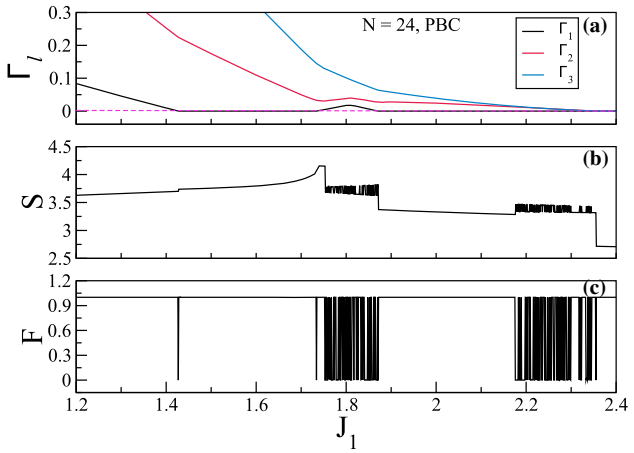

Fig. 7 **a** The spin gaps Γ_1, Γ_2 and Γ_3 are shown as a function of J_1 for 24 site spins in a 5/7 skewed ladder with PBC. For $J_1 < 1.427$, Γ_1 becomes nonzero and the system shows nonmagnetic behaviour. The system enters a reentrant nonmagnetic phase for $1.734 < J_1 < 1.872$ where Γ_1 is nonzero. The EE for the unsymmetrized GS is shown in (**b**), and the fidelity is shown in **c** as a function of J_1 for the unsymmetrized GS. The EE exhibits a discontinuous change, while fidelity shows a sharp drop at the transition points. Wild fluctuations (many transitions) in both the EE and fidelity around $J_1 = 1.8$ and 2.3 are due to the degeneracy in the GS energy

Table 2 The range of J_1 over which the GS have different symmetries in a 5/7 skewed ladder with $N = 24$ spins. The first column represents the range of J_1 for which the GS symmetry is $\sigma(+)$ and similarly the second column represents the GS is $\sigma(-)$ subspace. The third column gives the intervals of J_1 for which the GS is doubly degenerate

$\sigma(+)$	$\sigma(-)$	$\mid \Gamma_\sigma \mid = 0$
$1 < J_1 \leq 1.427$ and $1.871 < J_1 \leq 2.176$	$1.427 \leq J_1 \leq 1.753$ and $J_1 > 2.355$	$1.753 < J_1 \leq 1.871$ and $2.176 < J_1 \leq 2.355$

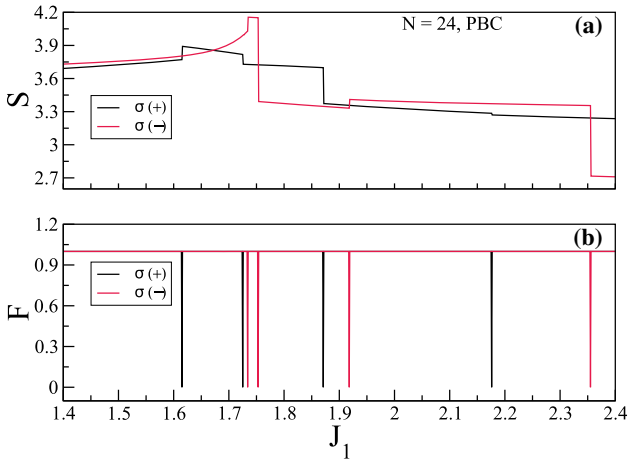

Fig. 8 For a 5/7 skewed ladder with 24 sites in PBC, **a** EE and **b** fidelity are plotted as a function of J_1 for both the reflection symmetry subspaces ($\sigma(+)$ and $\sigma(-)$). Black curve corresponds to the $\sigma(+)$ subspace, whereas the red curve represents the $\sigma(-)$ subspace

accompanied by vanishing of $|\Gamma_\sigma|$. EE shows a jump and fidelity shows a sharp dip at $J_1 = 1.615$ and 1.725. The change in EE and fidelity at 1.615 is associated with the maximum in the $|\Gamma_\sigma|$ gap. Beyond $J_1 = 1.615$, the $|\Gamma_\sigma|$ gap begins to close and at $J_1 = 1.754$ the gap vanishes. In region between 1.753 and 1.871, $|\Gamma_\sigma|$ vanishes. In the unsymmetrized calculations both fidelity and entropy show sharp fluctuations, which are suppressed when the degenerate ground states are obtained in the $\sigma(+)$ and $\sigma(-)$ subspaces (Fig. 8). In the J_1 region between 2.176 to 2.355 the GS is a spin triplet and $|\Gamma_\sigma|$ also vanishes. Fidelity of the $\sigma(+)$ and $\sigma(-)$ show a sharp dip at $J_1 = 2.176$ and 2.355 respectively; the GS below 2.176 has $\sigma(+)$ symmetry and becomes degenerate with the lowest state in $\sigma(-)$ symmetry in the region of J_1 ($2.176 < J_1 \leq 2.355$) and for J_1 value above 2.355 the GS switches back to $\sigma(-)$ subspace. There are no sharp changes in either entropy or fidelity beyond $J_1 = 2.355$.

5 Summary

We have studied EE and fidelity to characterize the quantum phase transitions in skewed ladder systems. While correlation function also give a measure of the extent of interactions between sites, EE embodies long range correlation between different parts of the system. In the regions of J_1 where the system has a nondegenerate GS without change in spin or spatial symmetry the entropy change is gradual and fidelity remains at one. At the transition points, the entropy shows a discontinuous change and fidelity shows a sharp dip. The transition points are accurately determined from these characteristic changes. In regions where the GS is degenerate, the unsymmetrized calculations show sharp fluctuations in EE and fidelity. However, in the symmetrized calculations they show abrupt changes only at the transition. We also find that for regions where $|\Gamma_\sigma|$ vanishes, the fidelity does not change in either subspace. But at the beginning and at the end of the transition, fidelity shows sharp dip in the lowest eigenstate of one of the symmetry subspaces.

Acknowledgements. S. Ramasesha acknowledges the Indian National Science Academy and DST-SERB for supporting this work. Manoranjan Kumar acknowledges the SERB for financial support through Project File No. CRG/2020/000754.

Author contributions

The project was conceived by S. Ramasesha and Manoranjan Kumar. Sambunath Das and Dayasindhu Dey have performed the numerical calculations. All the authors were involved in designing the calculations and interpretation of results. The work was jointly written up by all the authors.

Data Availibility Statement This manuscript has no associated data or the data will not be deposited. [Authors' comment: The data that support the findings of this study are available from the corresponding author upon reasonable request.]

References

1. C.K. Majumdar, D.K. Ghosh, On next-nearest-neighbor interaction in linear chain. ii. J. Math. Phys. **10**(8), 1399–1402 (1969). https://doi.org/10.1063/1.1664979
2. A.V. Chubukov, Chiral, nematic, and dimer states in quantum spin chains. Phys. Rev. B **44**, 4693–4696 (1991). https://doi.org/10.1103/PhysRevB.44.4693
3. R. Chitra, S. Pati, H.R. Krishnamurthy, D. Sen, S. Ramasesha, Density-matrix renormalization-group studies of the spin-1/2 heisenberg system with dimerization and frustration. Phys. Rev. B **52**, 6581–6587 (1995). https://doi.org/10.1103/PhysRevB.52.6581
4. S.R. White, I. Affleck, Dimerization and incommensurate spiral spin correlations in the zigzag spin chain: analogies to the kondo lattice. Phys. Rev. B **54**, 9862–9869 (1996). https://doi.org/10.1103/PhysRevB.54.9862
5. C. Itoi, S. Qin, Strongly reduced gap in the zigzag spin chain with a ferromagnetic interchain coupling. Phys. Rev. B **63**, 224–423 (2001). https://doi.org/10.1103/PhysRevB.63.224423
6. S. Mahdavifar, Numerical study of the frustrated ferromagnetic spin-1/2 chain. J. Phys. Condens. Matter **20**(33), 335–430 (2008). https://doi.org/10.1088/0953-8984/20/33/335230
7. J. Sirker, Thermodynamics of multiferroic spin chains. Phys. Rev. B **81**, 014–419 (2010). https://doi.org/10.1103/PhysRevB.81.014419
8. M. Kumar, A. Parvej, Z.G. Soos, Level crossing, spin structure factor and quantum phases of the frustrated

spin-1/2 chain with first and second neighbor exchange. J. Phys. Conden. Matter **27**(31), 316001 (2015). https://doi.org/10.1088/0953-8984/27/31/316001
9. Z.G. Soos, A. Parvej, M. Kumar, Numerical study of incommensurate and decoupled phases of spin-1/2 chains with isotropic exchange J_1, J_2 between first and second neighbors. J. Phys. Condensed Matter. **28**(17), 175603 (2016). https://doi.org/10.1088/0953-8984/28/17/175603
10. M. Kumar, S. Ramasesha, Z.G. Soos, Bond-order wave phase, spin solitons, and thermodynamics of a frustrated linear spin-$\frac{1}{2}$ heisenberg antiferromagnet. Phys. Rev. B **81**, 054413 (2010). https://doi.org/10.1103/PhysRevB.81.054413
11. T. Hamada, J.i. Kane, S.i. Nakagawa, Y. Natsume, Exact solution of ground state for uniformly distributed rvb in one-dimensional spin-1/2 heisenberg systems with frustration. J. Phys. Soc. Jpn. **57**(6), 1891–1894 (1988). https://doi.org/10.1143/JPSJ.57.1891
12. M. Kumar, B.J. Topham, R. Yu, Q.B.D. Ha, Z.G. Soos, Magnetic susceptibility of alkali-tetracyanoquinodimethane salts and extended hubbard models with bond order and charge density wave phases. J. Chem. Phys. **134**(23), 234304 (2011). https://doi.org/10.1063/1.3598952
13. M. Kumar, S. Ramasesha, Z.G. Soos, Tuning the bond-order wave phase in the half-filled extended hubbard model. Phys. Rev. B **79**, 035102 (2009). https://doi.org/10.1103/PhysRevB.79.035102
14. J.E. Hirsch, Charge-density-wave to spin-density-wave transition in the extended hubbard model. Phys. Rev. Lett. **53**, 2327–2330 (1984). https://doi.org/10.1103/PhysRevLett.53.2327
15. J.E. Hirsch, Phase diagram of the one-dimensional molecular-crystal model with coulomb interactions: half-filled-band sector. Phys. Rev. B **31**, 6022–6031 (1985). https://doi.org/10.1103/PhysRevB.31.6022
16. D. Dey, M. Kumar, Z.G. Soos, Boundary-induced spin-density waves in linear heisenberg antiferromagnetic spin chains with $s \geq 1$. Phys. Rev. B **94**, 144417 (2016). https://doi.org/10.1103/PhysRevB.94.144417
17. S.R. White, D.A. Huse, Numerical renormalization-group study of low-lying eigenstates of the antiferromagnetic s=1 heisenberg chain. Phys. Rev. B **48**, 3844–3852 (1993). https://doi.org/10.1103/PhysRevB.48.3844
18. E.S. So/rensen, I. Affleck, Equal-time correlations in haldane-gap antiferromagnets. Phys. Rev. B **49**, 15771–15788 (1994). https://doi.org/10.1103/PhysRevB.49.15771
19. T. Hikihara, L. Kecke, T. Momoi, A. Furusaki, Vector chiral and multipolar orders in the spin-$\frac{1}{2}$ frustrated ferromagnetic chain in magnetic field. Phys. Rev. B **78**, 144404 (2008). https://doi.org/10.1103/PhysRevB.78.144404
20. J. Sudan, A. Lüscher, A.M. Läuchli, Emergent multipolar spin correlations in a fluctuating spiral: The frustrated ferromagnetic spin-$\frac{1}{2}$ heisenberg chain in a magnetic field. Phys. Rev. B **80**, 140402 (2009). https://doi.org/10.1103/PhysRevB.80.140402
21. A. Parvej, M. Kumar, Degeneracies and exotic phases in an isotropic frustrated spin-1/2 chain. J. Magnet. Magn. Mater. **401**, 96–101 (2016). https://doi.org/10.1016/j.jmmm.2015.10.017
22. I. Affleck, T. Kennedy, E.H. Lieb, H. Tasaki, Rigorous results on valence-bond ground states in antiferromagnets. Phys. Rev. Lett. **59**, 799–802 (1987). https://doi.org/10.1103/PhysRevLett.59.799
23. I. Affleck, T. Kennedy, E.H. Lieb, H. Tasaki, Rigorous results on valence-bond ground states in antiferromagnets. Commun. Math. Phys. **115**, 477–528 (1988). https://doi.org/10.1007/BF01218021
24. U. Schollwöck, O. Golinelli, T. Jolicœur, S = 2 antiferromagnetic quantum spin chain. Phys. Rev. B **54**, 4038–4051 (1996). https://doi.org/10.1103/PhysRevB.54.4038
25. Z.C. Gu, X.G. Wen, Tensor-entanglement-filtering renormalization approach and symmetry-protected topological order. Phys. Rev. B **80**, 155131 (2009). https://doi.org/10.1103/PhysRevB.80.155131
26. F. Pollmann, E. Berg, A.M. Turner, M. Oshikawa, Symmetry protection of topological phases in one-dimensional quantum spin systems. Phys. Rev. B **85**, 075125 (2012). https://doi.org/10.1103/PhysRevB.85.075125
27. F. Haldane, Continuum dynamics of the 1-d heisenberg antiferromagnet: identification with the o(3) nonlinear sigma model. Phys. Lett. A **93**(9), 464–468 (1983). https://doi.org/10.1016/0375-9601(83)90631-X
28. F.D.M. Haldane, Model for a quantum hall effect without landau levels: condensed-matter realization of the "parity anomaly." Phys. Rev. Lett. **61**, 2015–2018 (1988). https://doi.org/10.1103/PhysRevLett.61.2015
29. H. Kikuchi, Y. Fujii, M. Chiba, S. Mitsudo, T. Idehara, T. Tonegawa, K. Okamoto, T. Sakai, T. Kuwai, H. Ohta, Experimental observation of the 1/3 magnetization plateau in the diamond-chain compound $cu_3(co_3)_2(OH)_2$. Phys. Rev. Lett. **94**, 227201 (2005). https://doi.org/10.1103/PhysRevLett.94.227201
30. H. Kikuchi, Y. Fujii, M. Chiba, S. Mitsudo, T. Idehara, T. Tonegawa, K. Okamoto, T. Sakai, T. Kuwai, H. Ohta, Kikuchi et al. reply. Phys. Rev. Lett. **97**, 089702 (2006). https://doi.org/10.1103/PhysRevLett.97.089702
31. B. Gu, G. Su, Comment on "experimental observation of the 1/3 magnetization plateau in the diamond-chain compound cu3(co3)2(OH)2. Phys. Rev. Lett. **97**, 563089 (2006)
32. M. Hase, M. Kohno, H. Kitazawa, N. Tsujii, O. Suzuki, K. Ozawa, G. Kido, M. Imai, X. Hu, 13 magnetization plateau observed in the spin-12 trimer chain compound $cu_3(P_2O_6H)_2$. Phys. Rev. B **73**, 104419 (2006). https://doi.org/10.1103/PhysRevB.73.104419
33. A. Maignan, V. Hardy, S. Hébert, M. Drillon, M.R. Lees, O. Petrenko, D.M.K. Paul, D. Khomskii, Quantum tunneling of the magnetization in the ising chain compound ca3co2o6. J. Mater. Chem. **14**, 1231–1234 (2004). https://doi.org/10.1039/B316717H
34. V. Hardy, D. Flahaut, M.R. Lees, O.A. Petrenko, Magnetic quantum tunneling in $ca_3co_2o_6$ studied by ac susceptibility: temperature and magnetic-field dependence of the spin-relaxation time. Phys. Rev. B **70**, 214439 (2004). https://doi.org/10.1103/PhysRevB.70.214439
35. V. Hardy, C. Martin, G. Martinet, G. André, Magnetism of the geometrically frustrated spin-chain compound sr_3HoCro_6: magnetic and heat capacity measurements and neutron powder diffraction. Phys. Rev. B

74, 064413 (2006). https://doi.org/10.1103/PhysRevB.74.064413
36. S. Ishiwata, D. Wang, T. Saito, M. Takano, High-pressure synthesis and structure of srco6o11: pillared kagomé lattice system with a 1/3 magnetization plateau. Chem. Mater. **17**(11), 2789–2791 (2005). https://doi.org/10.1021/cm050657p
37. X.X. Wang, J.J. Li, Y.G. Shi, Y. Tsujimoto, Y.F. Guo, S.B. Zhang, Y. Matsushita, M. Tanaka, Y. Katsuya, K. Kobayashi, K. Yamaura, E. Takayama-Muromachi, Structure and magnetism of the postlayered perovskite $sr_3co_2o_6$: a possible frustrated spin-chain material. Phys. Rev. B **83**, 100410 (2011). https://doi.org/10.1103/PhysRevB.83.100410
38. X. Yao, 1/3 magnetization plateau induced by magnetic field in monoclinic cov2o6. J. Phys. Chem. A **116**(9), 2278–2282 (2012). https://doi.org/10.1021/jp209830b. (**PMID: 22364513**)
39. M. Lenertz, J. Alaria, D. Stoeffler, S. Colis, A. Dinia, Magnetic properties of low-dimensional and cov2o6. J. Phys. Chem. C **115**(34), 17190–17196 (2011). https://doi.org/10.1021/jp2053772
40. Z. He, J.I. Yamaura, Y. Ueda, W. Cheng, Cov2o6 single crystals grown in a closed crucible: unusual magnetic behaviors with large anisotropy and 1/3 magnetization plateau. J. Am. Chem. Soc. **131**(22), 7554–7555 (2009). https://doi.org/10.1021/ja902623b. (**PMID: 19489641**)
41. W. Shiramura, K.i. Takatsu, B. Kurniawan, H. Tanaka, H. Uekusa, Y. Ohashi, K. Takizawa, H. Mitamura, T. Goto, Magnetization plateaus in nh 4cucl 3. J. Phys. Soci. Jpn. **67**(5), 1548–1551 (1998). https://doi.org/10.1143/JPSJ.67.1548
42. E. Dagotto, Complexity in strongly correlated electronic systems. Science **309**(5732), 257–262 (2005). https://doi.org/10.1126/science.1107559
43. G. Castilla, S. Chakravarty, V.J. Emery, Quantum magnetism of $cugeo_3$. Phys. Rev. Lett. **75**, 1823–1826 (1995). https://doi.org/10.1103/PhysRevLett.75.1823
44. G. Giri, D. Dey, M. Kumar, S. Ramasesha, Z.G. Soos, Quantum phases of frustrated two-leg spin-$\frac{1}{2}$ ladders with skewed rungs. Phys. Rev. B **95**, 224408 (2017). https://doi.org/10.1103/PhysRevB.95.224408
45. D. Dey, S. Das, M. Kumar, S. Ramasesha, Magnetization plateaus of spin-$\frac{1}{2}$ system on a 5/7 skewed ladder. Phys. Rev. B **101**, 195110 (2020). https://doi.org/10.1103/PhysRevB.101.195110
46. S. Das, D. Dey, M. Kumar, S. Ramasesha, Quantum phases of a frustrated spin-1 system: the 5/7 skewed ladder. Phys. Rev. B **104**, 125–138 (2021). https://doi.org/10.1103/PhysRevB.104.125138
47. S. Das, D. Dey, S. Ramasesha, M. Kumar, Quantum phases of spin-1 system on 3/4 and 3/5 skewed ladders. J. Appl. Phys. **129**(22), 223–902 (2021). https://doi.org/10.1063/5.0048811
48. M. Oshikawa, M. Yamanaka, I. Affleck, magnetization plateaus in spin chains: "haldane gap" for half-integer spins. Phys. Rev. Lett. **78**, 1984–1987 (1997). https://doi.org/10.1103/PhysRevLett.78.1984
49. Y.C. Li, Y.H. Zhu, Z.G. Yuan, Entanglement entropy and the Berezinskii–Kosterlitz–Thouless phase transition in the j1–j2 heisenberg chain. Phys. Lett. A **380**(9), 1066–1070 (2016). https://doi.org/10.1016/j.physleta.2016.01.004
50. D.W. Luo, J.B. Xu, Quantum phase transition by employing trace distance along with the density matrix renormalization group. Ann. Phys. **354**, 298–305 (2015). https://doi.org/10.1016/j.aop.2014.12.023
51. S.J. Gu, Fidelity approach to quantum phase transitions. Int. J. Mod. Phys. B **24**(23), 4371–4458 (2010). https://doi.org/10.1142/S0217979210056335
52. D. Petz, *Entropy, von Neumann and the von Neumann Entropy* (Springer Netherlands, Dordrecht, 2001), pp. 83–96. https://doi.org/10.1007/978-94-017-2012-0_7
53. A. Rényi, On measures of entropy and information. In: Proceedings of the 4th Berkeley Symposium on Mathematics, Statistics and Probability, **1**, 547–561 (1961)
54. V.M.L.D.P. Goli, S. Sahoo, S. Ramasesha, D. Sen, Quantum phases of dimerized and frustrated heisenberg spin chains withs= 1/2, 1 and 3/2: an entanglement entropy and fidelity study. J. Phys. Conden. Matter **25**(12), 125–603 (2013). https://doi.org/10.1088/0953-8984/25/12/125603
55. A.B. Kallin, I. González, M.B. Hastings, R.G. Melko, Valence bond and von neumann entanglement entropy in heisenberg ladders. Phys. Rev. Lett. **103**, 117–203 (2009). https://doi.org/10.1103/PhysRevLett.103.117203
56. M. Thesberg, E.S. Sørensen, General quantum fidelity susceptibilities for the $J_1 - J_2$ chain. Phys. Rev. B **84**, 224–435 (2011). https://doi.org/10.1103/PhysRevB.84.224435
57. S. Chen, L. Wang, S.J. Gu, Y. Wang, Fidelity and quantum phase transition for the heisenberg chain with next-nearest-neighbor interaction. Phys. Rev. E **76**, 061–108 (2007). https://doi.org/10.1103/PhysRevE.76.061108